Implementing Rational Surface Locations Measured From Thomson Scattering Into MSTfit

by

Curtis A. Johnson

Senior Thesis

(Physics)

at the

University of Wisconsin-Madison

2014

Abstract

Measurements of rational surface (RS) locations in the Madison Symmetric Torus as measured by Thomson Scattering (TS) have been implemented in the equilibrium reconstruction program MSTfit. Possible correlated errors between diagnostics show a small impact on the equilibrium reconstruction done by MSTfit. TS RS locations have shown to be a good constraint on the equilibrium. The addition of Thomson Scattering leads to the reduction of the χ^2, and more physical results for some equilibrium models as well as a decrease in error bars of parameter profiles. A reduction in the q-profile has been shown to be associated with the presence of neutral beam injection. This is consistent with the suppression of tearing modes.

Acknowledgements

There are a few people whose work made this thesis possible. First, I would like thank Eli Parke. Without his help and guidance, this work would not have been possible. This thesis is based off work that he has done. Dr. Jay Anderson provided much help in this endeavor, without his expertise on MSTfit I would not have been able to complete this endeavor. I would also like to thank my adviser Dr. Daniel Den Hartog for making this thesis a possibility for me. Much of this thesis is also based off work done by Hilary Stephens. I would like to thank Dr. Josh Reusch for his patience in helping me to implement MSTfit on the blade severs. I would also like to thank both the TS and IDA groups. Finally, I would like to thank Lynn Johnson for helping to edit to this thesis.

Contents

List of Tables

List of Figures

Chapter 1

Introduction

The Madison Symmetric Torus (MST) is a reversed field pinch (RFP) magnetic confinement plasma device. The RFP is a toroidal geometry device used in fusion research. A basic diagram of the RFP is shown in Figure 1. In a general discharge, a puff of deuterium gas is squirted into the device along with a few loose electrons, a toroidal magnetic field is created by current driven through the aluminum shell, which in turn creates an initial plasma in the device. This plasma is then driven by pulsing the transformer as shown in Figure 1.1.

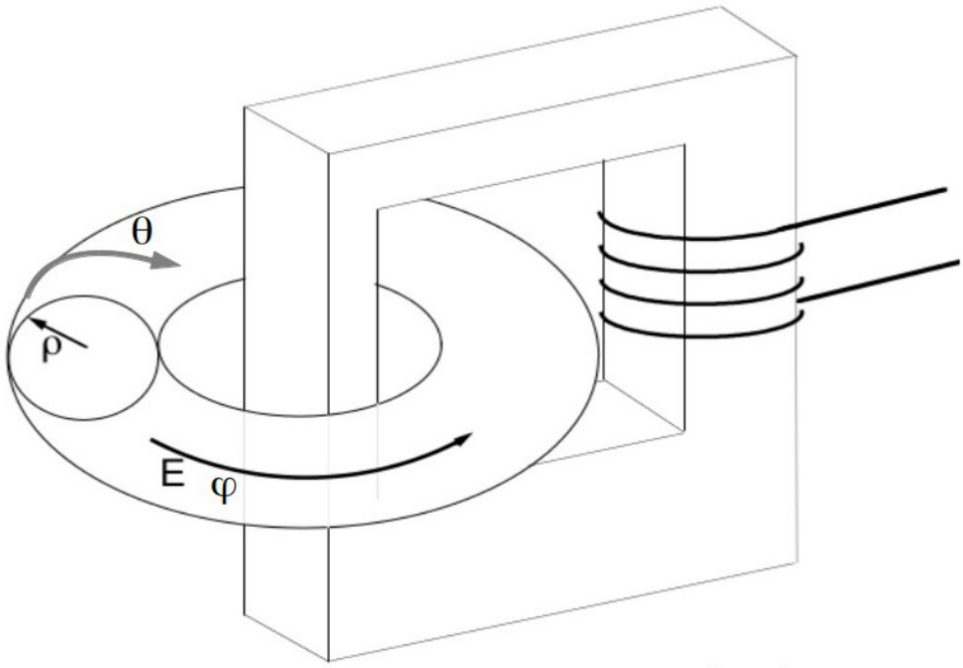

Figure 1.1. Basic sketch of RFP. Where θ is the poloidal direction, φ is the toroidal direction, ρ is the radial direction and E is the electric field.

The plasma acts like an ordinary secondary of a transformer driving current through the plasma. The driven toroidal current then creates a poloidal magnetic field. This field is similar in strength to that of the external toroidal field. In a typical RFP discharge, the toroidal magnetic field decreases from the core to the edge of the plasma. The toroidal magnetic field is eventually reversed at the edge giving the

RFP its name. Magnetic field profiles for a typical discharge are shown in Figure 1.2.

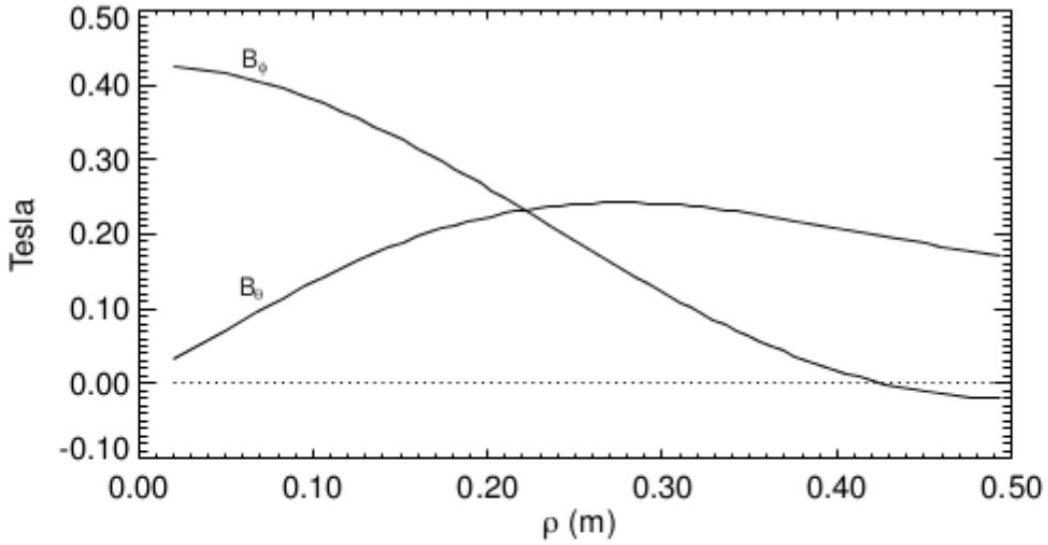

Figure 1.2. Magnetic field profiles of a typical RFP discharge. Courtesy of Jay Anderson

Neutral Beam Injection

Neutral beam injection on MST is done with a 25 kV 50 A hydrogen beam. The use of NBI in MST creates a core localized population of fast ions. The addition of fast ions into MST can modify the current profile from conditions without NBI. The change in current profile has important implications for plasma equilibrium and mode stability. It is this reason that NBI is important to this body of work .

Equilibrium Reconstruction

In many plasma devices, there is often a lack of total diagnostic coverage. Diagnostics also do not provide complete internal measurements of the plasma. The use of magneto hydrodynamic (MHD) consistent equilibria can be calculated and fit to iteratively to match the measured data. The use of these equilibria can off set the lack of total diagnostic coverage. Equilibrium reconstructions can be used to evaluate the impact of NBI on current profiles.

1.1 Thesis Overview

In this thesis, rational surface (RS) locations for tearing modes as found from the Thomson Scattering (TS) diagnostic are integrated into the equilibrium reconstruction routine MSTfit. The impact of this new constraint on the equilibrium is investigated. Chapter 1 introduces the TS diagnostic as well as MSTfit. Chapter 2 gives an overview of temperature fluctuations and the fitting routine. The incorporation of TS RS locations into MSTfit is discussed. Chapter 3 gives an overview of the impact of this new constraint on the equilibrium profiles as well as an apparent decrease in the q-profile on axis with the presence of NBI.

1.2 Thomson Scattering Diagnostic

Electron temperature measurements are taken with a multi-point Thomson scattering diagnostic. Linearly polarized laser light is pulsed vertically through MST. The laser light interacts through the Lorentz force with electrons. The electrons of the plasma in MST are relativistic electrons are accelerated at significant speeds. Thomson scattering approximation is valid when photon energy is less than the rest mass of an electron but E_{laser} B_{laser} are large, leading to a strong acceleration. While this is needed for the diagnostic application of the lasers, this required does not have to be met In general. Light radiates from the interaction with the electron with both temperature and density information. The total intensity of scattered light is proportional to the density. The temperature of plasma is proportional to the width of the photon spectrum. The increase in width is a result of the doppler shift of the laser Light by the electrons. Photons in MST come from two Spectron ND:YAG lasers operating at 1064 nm and 9 ns FWHM pulse duration. There is also a new fast Thomson scattering system operating at 1064 nm and allows for 50 kHz operation. The faster operation allows for more data to be ensembled resulting in decreased error bars. The decrease in error bars is potentially valuable for the work described here as ensembles of many shots are required. This new TS system has not yet been used for tearing mode correlations.

The light is collected with fiber optic bundles from 21 different radial locations shown in Figure 1.3. Collected light is sent to six-channel polychromators, polychromators bin scattered light into different spectral channels for measuring the width of the spectrum. Photons are then converted to a voltage signal with a avalanche photodiode, then amplified, and then digitized. Bayesian analysis is used to infer T_e and n_e with associated errors based on the distribution of scattered and background light on each channel.

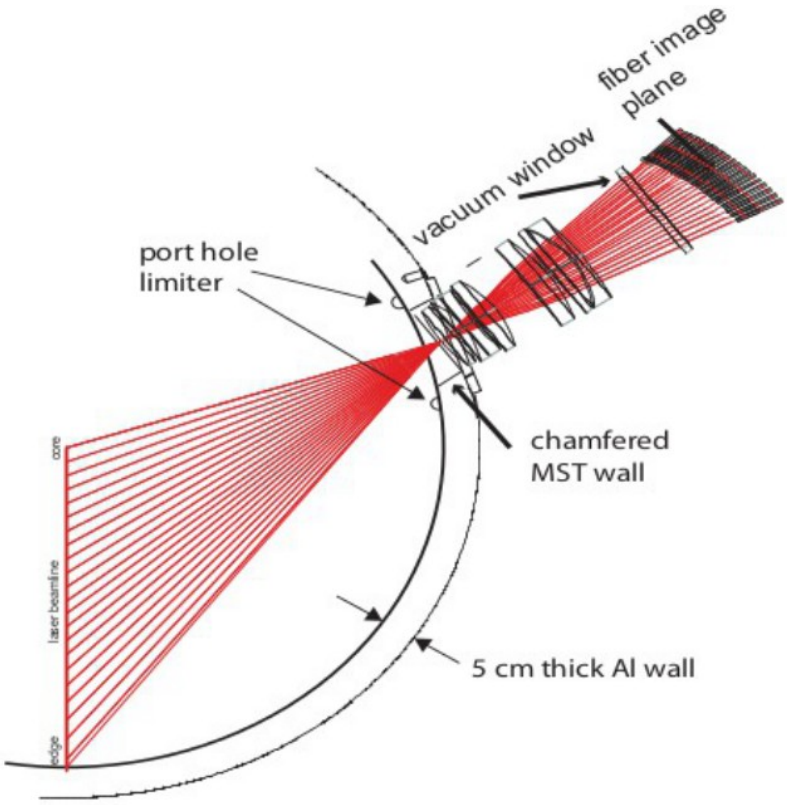

Figure 1.3. Schematic of the radial positions available to the fiber optic bundles. Courtesy of H. Stephens

1.3 Equilibrium Reconstruction Program MSTFit

MSTfit is a nonlinear Grad-Shafranov equation solver; the code finds a solution to the Grad Shafranov equation[1].

$$J_\varphi = \frac{2\pi FF'}{\mu_0 R} + 2\pi Rp' \qquad (1)$$

Where $F = RB_\varphi = F(\psi)$, this specifies the current profile, pressure $p(\psi)$ is also a function of poloidal flux ψ. The solution to the equation is found on a two-dimensional grid. The close fitting aluminum shell is approximated as a constant flux boundary. The triangle mesh solution grid is that of Figure 1.4. The solution is specified by the free parameters F and P. The code varies these profiles to find the solution that bests fits the experimental data. The accuracy of the equilibrium is dependent on the data that is used to constrain the equilibrium as well as the model that is selected. MSTfit assumes a modified polynomial function model as a first guess, then performs the Nelder-Mead downhill simplex method on the χ^2 comparing the predicted to observed diagnostic signals and changing the free parameters F and P accordingly. In a RFP, the pressure is not as large of a contributing factor as in other plasma devices such as the tokamak, and thus, the P parameter in MSTfit does not strongly constrain the equilibrium.

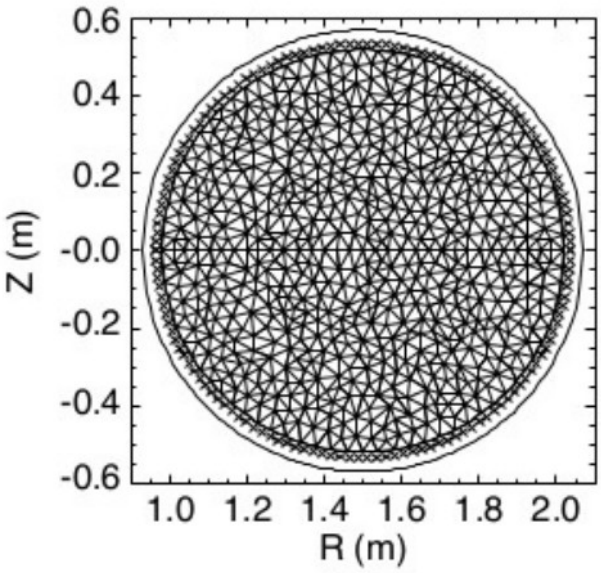

Figure 1.4. MSTfit solution grid, the Grad Shafranov equation is solved on this mesh. Courtesy of J.K. Anderson

Many diagnostics that are available to MST are incorporated into MSTfit. The current profiles in MSTfit are calculated with equations 1 and 2.

$$J_\theta = \frac{2\pi}{\mu_0} F' B_\theta \qquad (2)$$

Diagnostics that constrain F and F', the parameters that constrain the current profiles, have a greater impact on the equilibrium reconstruction than diagnostics that do not, such as those that constrain the pressure profile. The predicted diagnostic signals calculated from the free parameters are compared to the available plasma diagnostics and the Amoeba minimization is used to converge on free parameters that predict the given diagnostic signals. The free parameter profile is defined by a user chosen number of free knots; spline interpolation between these knots is used to construct the profiles. Restricting the number of free knots can greatly impact the solution and the variability of solutions for similar discharges and also the computational time required to arrive at a solution. MSTfit now uses a true reduced χ^2 value given by equation 3, where ν is the number of degrees of freedom in the reconstruction equal to the number of free data minus the number of knots in the free parameter, M is the predicted signal for the diagnostic, D is the data from the diagnostic, and σ is a one sigma standard deviation of the error in the measurement. This was chosen to aid in the determination of number of knots in the free parameter warranted by a reconstruction.

$$\chi^2_{red} \equiv \frac{1}{\nu} \sum_i \frac{\left(D_i - M_i\right)^2}{\sigma_i^2} \tag{3}$$

Weighting of different parameters is accomplished through the standard deviation σ. This eliminates any confusion introduced by a weighting term and serves to simplify the treatment of different diagnostics in the code.

Chapter 2

2.1 Temperature Fluctuation and Resonant Surfaces

In an RFP, the equilibrium field twists helically around the magnetic axis, the bending of the field lines is given by the safety factor q show in equation 4. Where r is the minor radius, R is the major Radius, and B is the magnetic field in the poloidal and toroidal directions.

$$q=\frac{rB_{\Phi}}{RB_{\theta}} \tag{4}$$

When the wave vector is perpendicular to the magnetic field, the magnetic fluctuations become resonant. Parameters m and n represent the poloidal and toroidal wavenumbers.

$$\frac{mB_{\theta}}{r}+\frac{nB_{\Phi}}{R}=0 \tag{5}$$

Using equation 5, the safety factor can be written as:

$$q(r)=-\frac{m}{n} \tag{6}$$

In a typical RFP discharge, q at the edge is generally less than 0. For the non-reversed plasmas in this work $q(a)\geq 0$. A typical q-profile is shown in Figure 2.1, the resonances specified by equation 5 are shown in this plot.

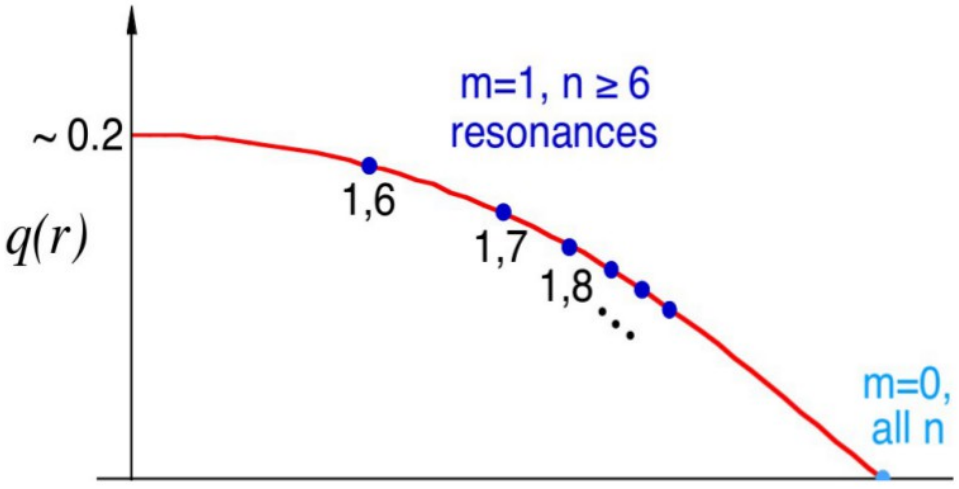

Figure 2.1. A typical q-profile for discharges used in this work. Courtesy of Hillary Stephens

Electron temperature fluctuations found with TS are detected through Bayesian analysis techniques that correlate electron temperature to magnetic fluctuations as measured from the toroidal array[2,7]. Electron temperature is modeled as a mean temperature with fluctuating temperature structure on top.

$$T_e(r) = T_{e0}(r) + \tilde{T}_{e,n}(r)\cos\Delta_{TS_n} \quad (4)$$

Where T_e is the measured electron temperature, T_{e0} is the mean electron temperature, $\tilde{T}_{e,n}$ is the fluctuation temperature, and Δ_{TS_n} is the phase of the magnetic fluctuation at the TS location. The phase information Δ_{TS_n} is needed because modes are rotating past the TS laser cord. The toroidal array is not at the same location as the TS diagnostic and thus Δ_{TS_n} also includes a correction for this offset. The relatively low number of T_e measurements in a plasma discharge, (6-8) measurements in a laser burst ~30 per discharge requires a Bayesian analysis to ensemble data together. A detailed explanation of this process is found in [2]. An isothermal temperature structure island produces cooler temperatures inside the resonant surfaces and higher temperatures in the surrounding plasma, the net effect of this is to flatten T_e across the island. Fluctuations will exhibit a phase flip across the resonant surface for the tearing mode [2,5]. This flip in sign allows for the location of the resonant surface to be found radially. It is this assumption that is at the core of this work to constrain the equilibrium reconstruction with TS RS. In Tokamak discharges, measurements are consistent with reconstructed q-profiles, this flip in sign occurs at the center of the rational surface[6]. This assumption is used here as well. The flip in sign of the temperature fluctuation designating the rational surface location is shown in figure 2.2. The rational surfaces locations used in this work are shown in Table 2.1.

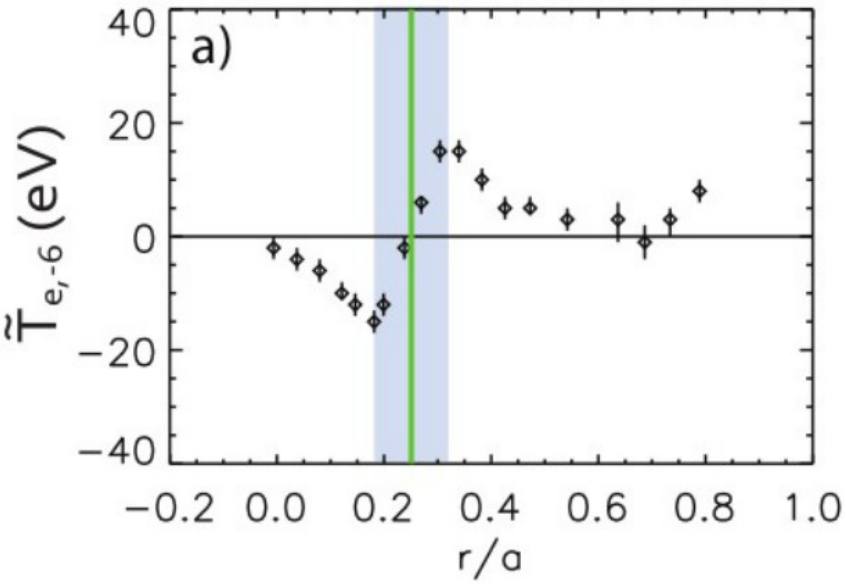

Figure 2.2. Electron temperature fluctuation amplitude associated with the m=1 n=-6 tearing mode designating the location of the center of the rational surface with the green line. Courtesy of Hillary Stephens

Rational Surface Number n	Radial Position of RS, NBI Absent [cm]	Radial Position of RS, NBI Present [cm]
6	19	17.5
7	24	25
8	27	28

Table 2.1. Locations of the n=6,7,8 rational surfaces measured by Thomson Scattering used in this work

2.2 Fitting Thomson Scattering Rational Surfaces

The implementation of fitting TS RS values in the program MSTfit by calculating B_{theta} and B_{phi} evaluated on the 2D solution grid as well as the flux surface average, this is important because the plasma rotation means TS measurements are also flux surface averaged and thus a local q-profile calculation can not be used. The q-profile from the flux surface average is projected onto the TS laser chord allowing direct measurements of rational surfaces from Thomson Scattering to be used. The q profile can be calculated in MSTfit with the following equation.

On each iteration of the fitting process the flux surface averaged q profile equation 5 is calculated. The flux Averaged q profile is then mapped to the Thomson viewing geometry. This determines the value of q at each possible measurement point.

$$q=\left\langle \frac{r\,B_{\varphi}}{R\,B_{\theta}} \right\rangle \tag{5}$$

Once the q profile is calculated with the free parameters F and P, the location of the n=6,7,8 surfaces are calculated and are then compared to the surface locations as measured by TS, and a χ^2 calculation is preformed which is fed back into the total χ^2 value like other diagnostics.

$$\chi^2=\sum_{i=6}^{8}\frac{\left(z_{data_i}-z_{fit_i}\right)^2}{\sigma_i^2} \tag{6}$$

Z_{fit} is the location of the MSTfit predicted rational surface (typically q= 1/6, 1/7, 1/8). Z_{data} is the measure zero crossing of the temperature fluctuation from Thomson Scattering data. Is the uncertainty in the measurement, related to the statistical noise in the T_e data and the spacing of view points.

Chapter 3

3.1 Equilibrium Uncertainty and Correlated Errors

One metric to judge the impact of TS RS values on the constraint of the reconstruction is to estimate the uncertainty in the equilibrium. If the RS values are a good constraint the uncertainty in the fit should be reduced as the values create a strong constraint on the equilibrium. An estimate to the uncertainty in the fit is done in a semi-analytic fashion in MSTFit by assuming the χ^2 quantity is a function of N free parameters. This can then be Taylor expanded about its minimum producing equation 7

$$\chi^2=\chi_0^2+\sum_{i=1}^{N}\frac{\partial\,\chi_0^2}{\partial\,a_i}+\frac{1}{2}\sum_{i=1}^{N}\sum_{j=1}^{N}\frac{\partial^2\chi_0^2}{\partial a_i\partial a_j}\delta a_i\delta a_j+O\left(\delta a^3\right) \tag{7}$$

where χ_0^2 is the function minimum, δa_i is the deviation of the i[th] free parameter from its value at the minimum. The value of χ^2 can be approximated as a quadratic in each free parameter because the first derivative at the minimum must be zero. The mixed partial derivatives of equation 7 will go to zero for free parameters that are uncorrelated. In the vicinity of the minimum value the assertion

$$\chi^2-\chi_0^2=v\,\delta a_i^2 \rightarrow \chi^2=v\,\delta a_i^2+c \rightarrow \chi^2=\frac{\delta a_i^2}{\sigma_i^2}+C \qquad (8)$$

holds where C is a function of all the other a_j . σ_i is the standard deviation of the fit parameter defined by $\sigma_i^2=2\left(\frac{\delta^2\chi^2}{\delta a}\right)^{-1}$ The code makes this approximation by tabulating χ^2 values versus each free parameter near the minimum which are fit to the quadratic equation 8 to determine the standard deviation in the free Parameter. A plot of the quadratic approximation is shown in Figure 3.1. χ_0^2 occurs at the lowest point on the surface.

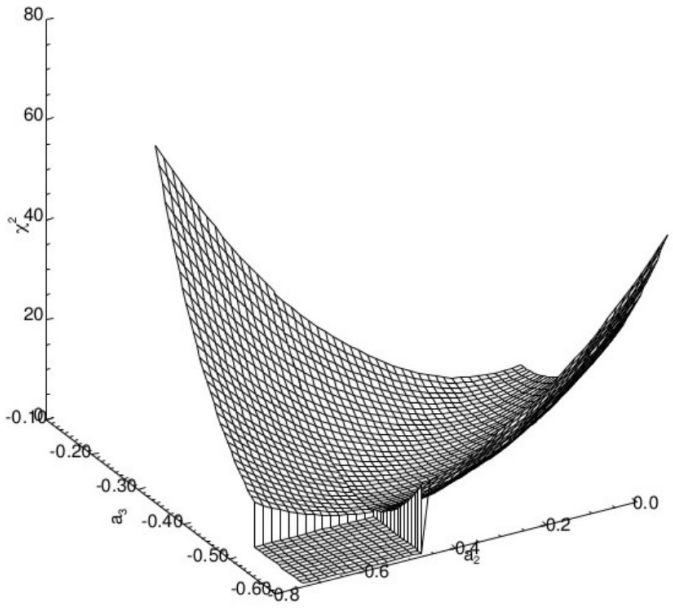

Figure 3.1. Graph of the quadratic approximation of the χ^2 used by MSTfit with two arbitrary parameters. Plot courtesy of J.K. Anderson.

This quadratic approximation method is computationally inexpensive when compared with other uncertainty estimations. The method, however, assumes that errors between diagnostics are uncorrelated. It has been noted that the presence of correlated errors in the equilibrium can lead to an

over estimation of the uncertainty in the reconstruction [3,4]. Finding and calculating correlated errors experimentally between diagnostics is an extremely difficult if not impossible task. If correlated errors are present between the diagnostics, there should be an over prediction in the error that is predicted by the quadratic approximation method when compared to the error calculated by ensembling large amounts of data. Taking real data in quantities that would be sufficient to do error analysis to compare to the quadratic fit of the χ^2 method would require prohibitively large ensembles and thus was not pursued. A method taking the diagnostic data from one shot and adding gaussian noise data within measured uncertainties for the discharge was pursued. Diagnostics that were varied included I_p the driven current in the shell of MST, toroidal flux the magnetic flux in the toroidal direction, r0b0 is a measurement of the edge magnetic field, b_0 the magnetic field on axis, and the B_p array the measurements of the poloidal magnetic field; a sample of this process is shown in Figure 3.2. To simulate an ensemble of data, 1000 different simulated signal discharges were put through the reconstruction. This method relied on the normal distribution and randomness to give a good sampling of the possible combinations that would occur in an ensemble of actual data.

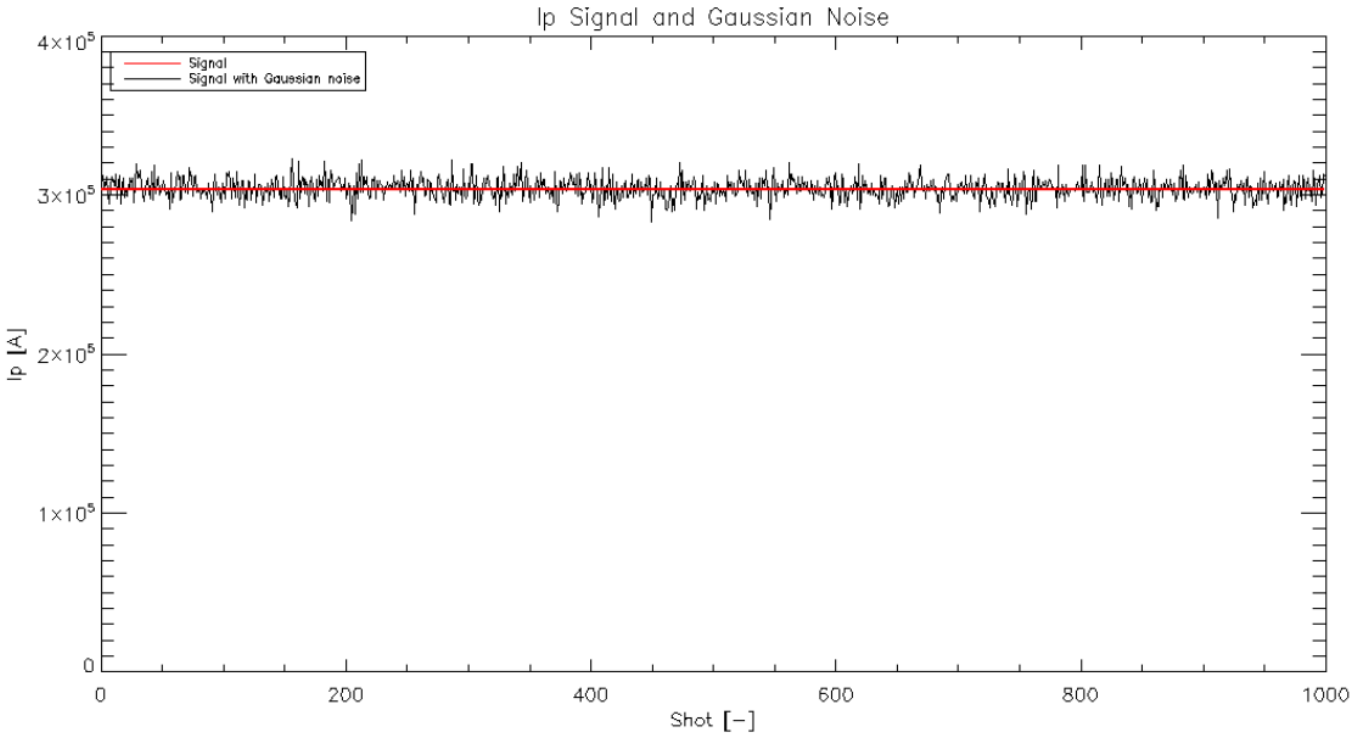

Figure 3.2. I_p signal with Gaussian noise to simulate an ensemble of data.

The method of creating reconstructions of 1000 different data is computationally expensive. A single reconstruction can take over five minutes to complete. Equilibrium reconstructions were run in parallel to allow for completion in a timely manner. After the fitting process was complete for the 1000 discharges with normal randomness included, the average and standard deviation of each parameter was tabulated. The envelope created by the standard deviation of the different profiles can then be compared to the envelope calculated by the quadratic fitting of the χ^2 method. As previously mentioned, the presence of correlated errors between the diagnostics could introduce error that would cause the quadratic method to over predict the envelope of the profiles significantly. As shown in Figure 3.3, the envelope for the quadratic method does not grossly over predict the errors for most plasma parameters when compared to the many reconstructions. Some profiles such as the poloidal

magnetic field and toroidal flux are over predictions but in general, most profiles do over predict to the degree of these measurements. Profiles such as the q-profile are good approximations. Before the new reduced χ^2 was used in the reconstruction, the quadratic method greatly over predicted the many reconstructions and was not a good approximation. The reduction in the envelope can be attributed to the new reduced χ^2 routine. The approximation through the quadratic method is a reasonable approximation for the computational time required as it takes approximately 20 times less computational resources than ensembles of reconstructions.

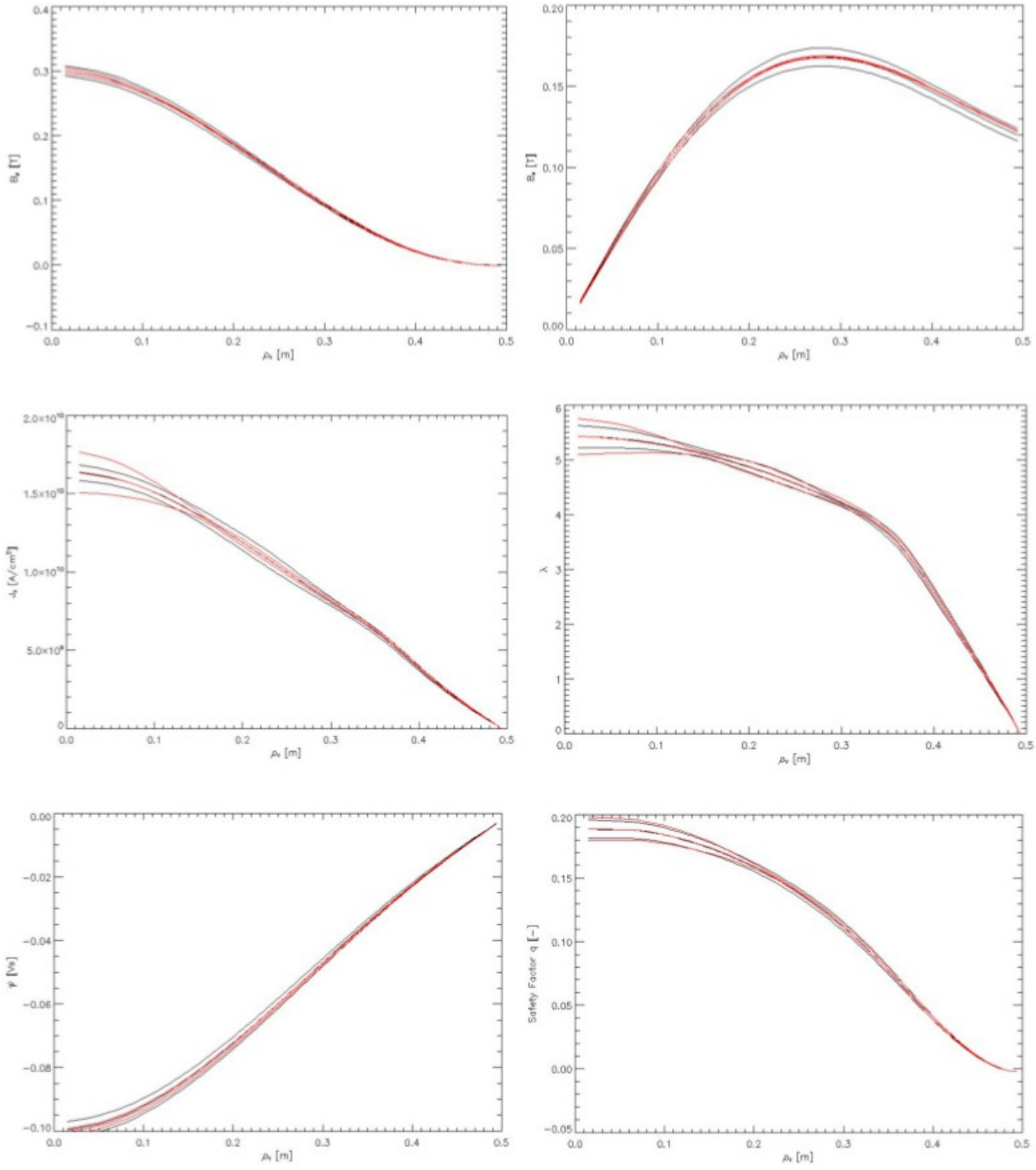

Figure 3.3. Uncertainty in computed equilibrium quantities shown in black and uncertainty of 1000 reconstructions shown in red. The envelope for computed quantities is computed by varying the free parameters slightly from the value at the minimum χ^2_{red} value. The envelopes from 1000 reconstructions are computed by taking the standard deviation of the 1000 reconstructions.

3.2 Choosing A Model For Fits

MSTfit offers two basic types of models that are investigated in this work. The number of knots in the free parameter F' are allowed to be specified as well as if the location of the knots are free or fixed. For N fixed knots, there are N-1 free parameters; with varying knot locations, the free parameters go as 2N-3. Figure 3.4 shows the use of 4 free knots like is done with the free parameter (F'). Figure 3.4 is a cartoon diagram to illustrate the fitting process it is not the F' profile but an arbitrary quadratic function. The end two knots shown in red have a fixed location but are free magnitude giving two free parameters. The blue knots are free to wander in both coordinates but are required not to switch places. This gives three free parameters, for a total of five free parameters.

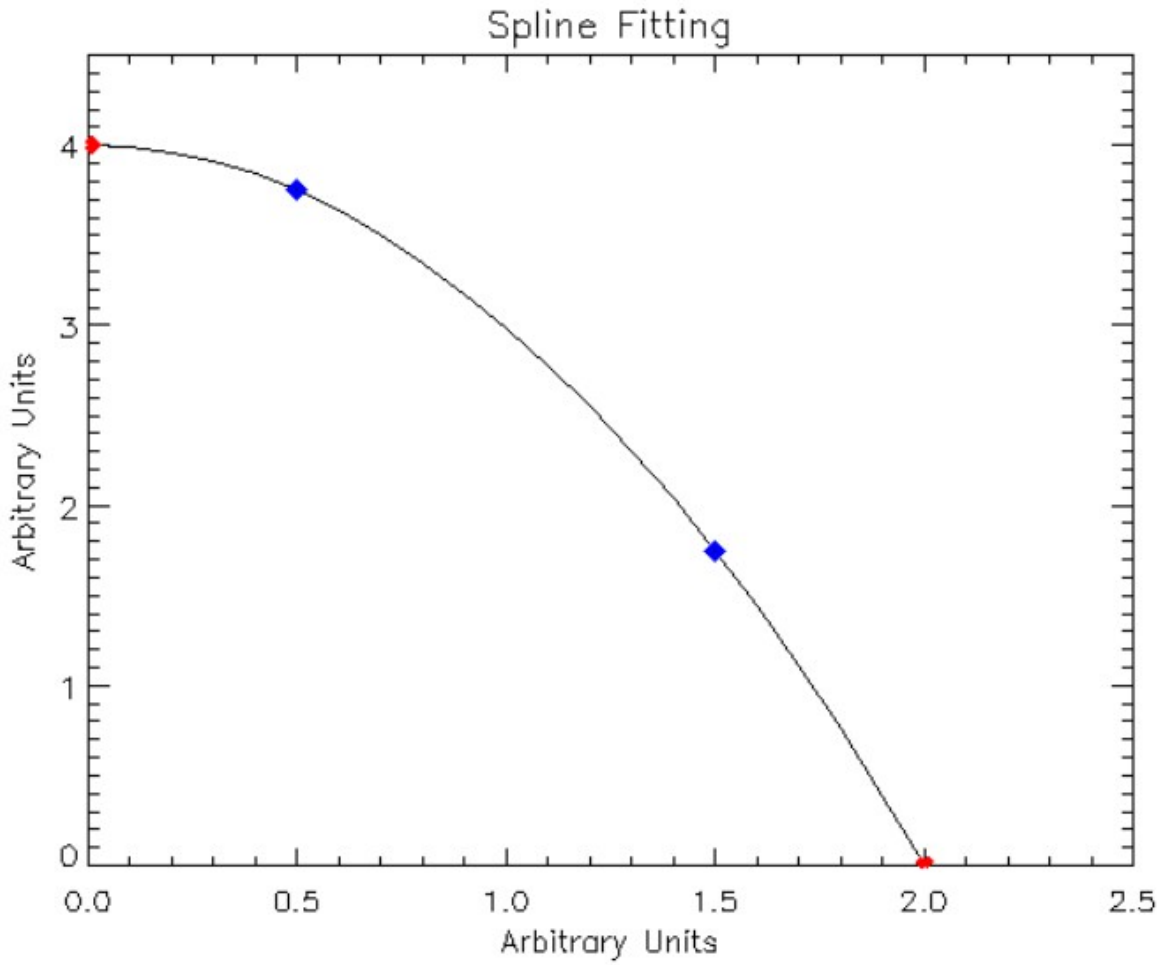

Figure 3.4. Spline fitting of knot locations to the free parameters of a quadratic function.

There are different free parameter models that are available to MSTfit. The number of free knots can be varied in MSTFit. The choice of knots can impact the equilibrium profile substantially. Figure 3.5 shows the q-profile for same MST shot using the ensemble 1000 normally varied discharges with three, four, and five free knots. The variability in the profile is quite substantial and highlights the importance of model selection. The best choice of model is the model that creates the smallest reduced χ^2 value as this is the model that best fits the available data. The addition of more free knots in the free parameters allows for more structure to be captured in the different profiles and thus is desirable. The number of free parameters in the F' profile increases with the number of knots as 2N-3. Free parameters may be added to the reconstruction if the reduced χ^2 value decreases by at least 15 percent [9]. The addition of TS RS locations into the reconstruction allows for the addition of a free parameter as the reduced χ^2 decreases by approximately half when going from three to four free knots as shown in Table 3.1.

Number of Free Knots No TS RS Locations	Mean χ^2_{red} for fits
Three	0.789
Four	0.631
Five	0.682

Number of Free Knots TS RS Locations Included	Mean χ^2_{red} for fits
Three	1.27
Four	0.74
Five	0.81

Table 3.1. Reduced χ^2 value for different models of same discharge conditions.

This reduction in the reduced χ^2 would suggest that the TS RS location values are good constraints on the equilibrium and benefit the equilibrium as more free knots are able to be added to the equilibrium reconstruction. The reduced χ^2 values presented here are less than one; this would suggest that the model is over fitting the data. The most reasonable explanation for this is that the error of diagnostics is an over estimation as the reduced χ^2 is inversely proportional to the square of the standard deviation of the error in the measurement as show in equation 2. The poloidal error estimation is the most likely culprit as the source of this error. However, the source of error was not investigated as the model selection does not depend on the absolute value, just the relative values between the number of free knots.

The q-profiles corresponding to these different models are shown in the figures below. Profiles are shown with different models including and excluding TS RS values. When RS locations are not included, the addition of more free parameters causes the q profile to flatten in the core and become less than 0.2 on axis. This low and flat q profile is not expected for the discharge parameters of the shot as shown in Figures 3.5 and 3.6. The increase in free parameters is also not accompanied by the decrease in the reduced χ^2. The standard deviation in the q profile also increases with the number of free parameters suggesting that there is more freedom in the equilibrium that is not warranted, allowing for many different q profiles to be constructed from the same plasma discharges. When TS RS locations are added to the equilibrium, the q profiles are steepened and increased in the core. This is more in line with the expected outcome from the discharge parameters. The standard deviation in the q-profile also decreases indicating that the addition of TS RS values allows for four free parameters in the F' profile. From the graphs, it is clear that at most 3 knots can be used if realistic reconstructions are desired and TS RS locations are not included in the reconstruction.

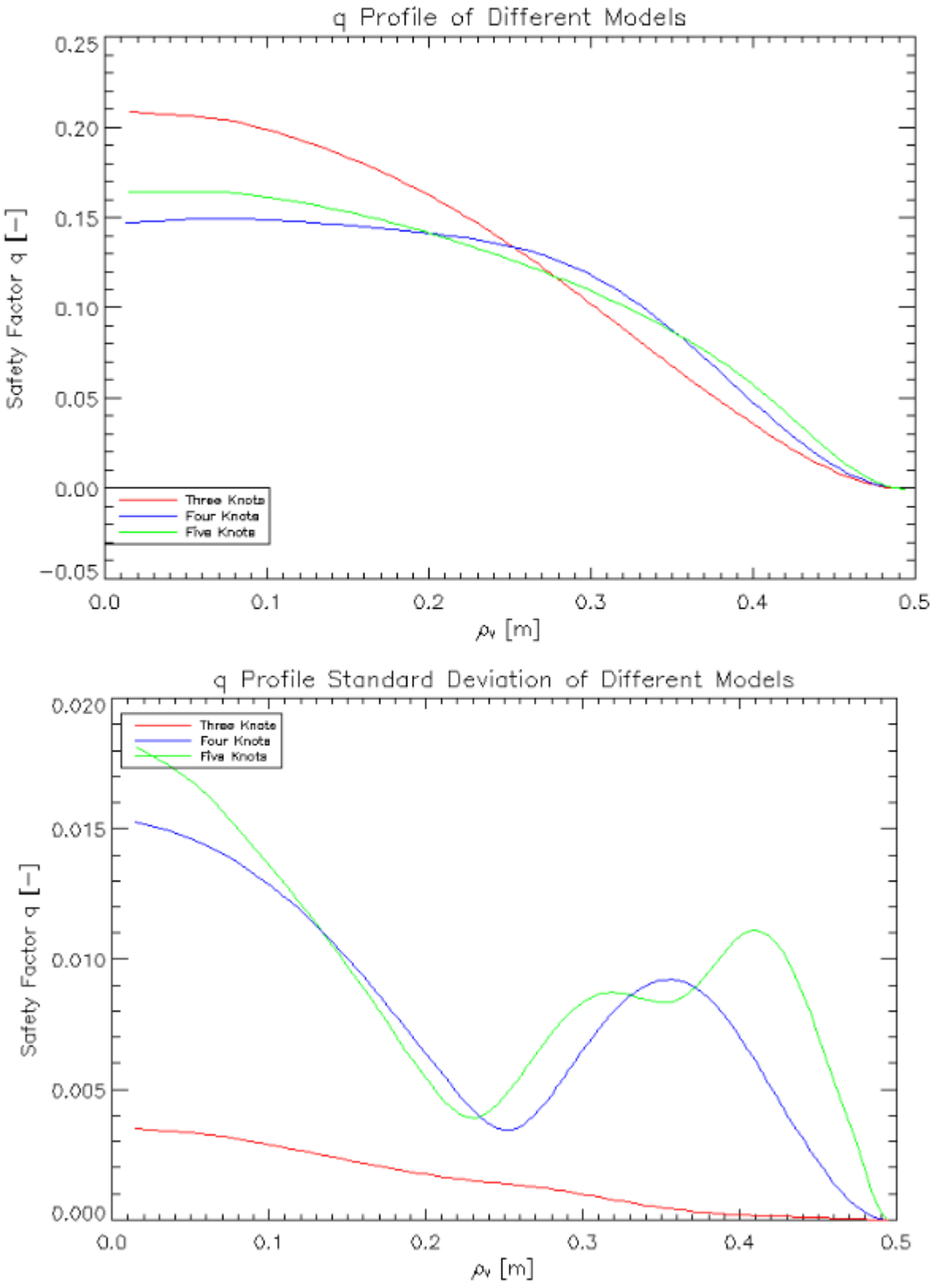

Figure 3.5. q-profile and standard deviation of profile with no TS RS location included.

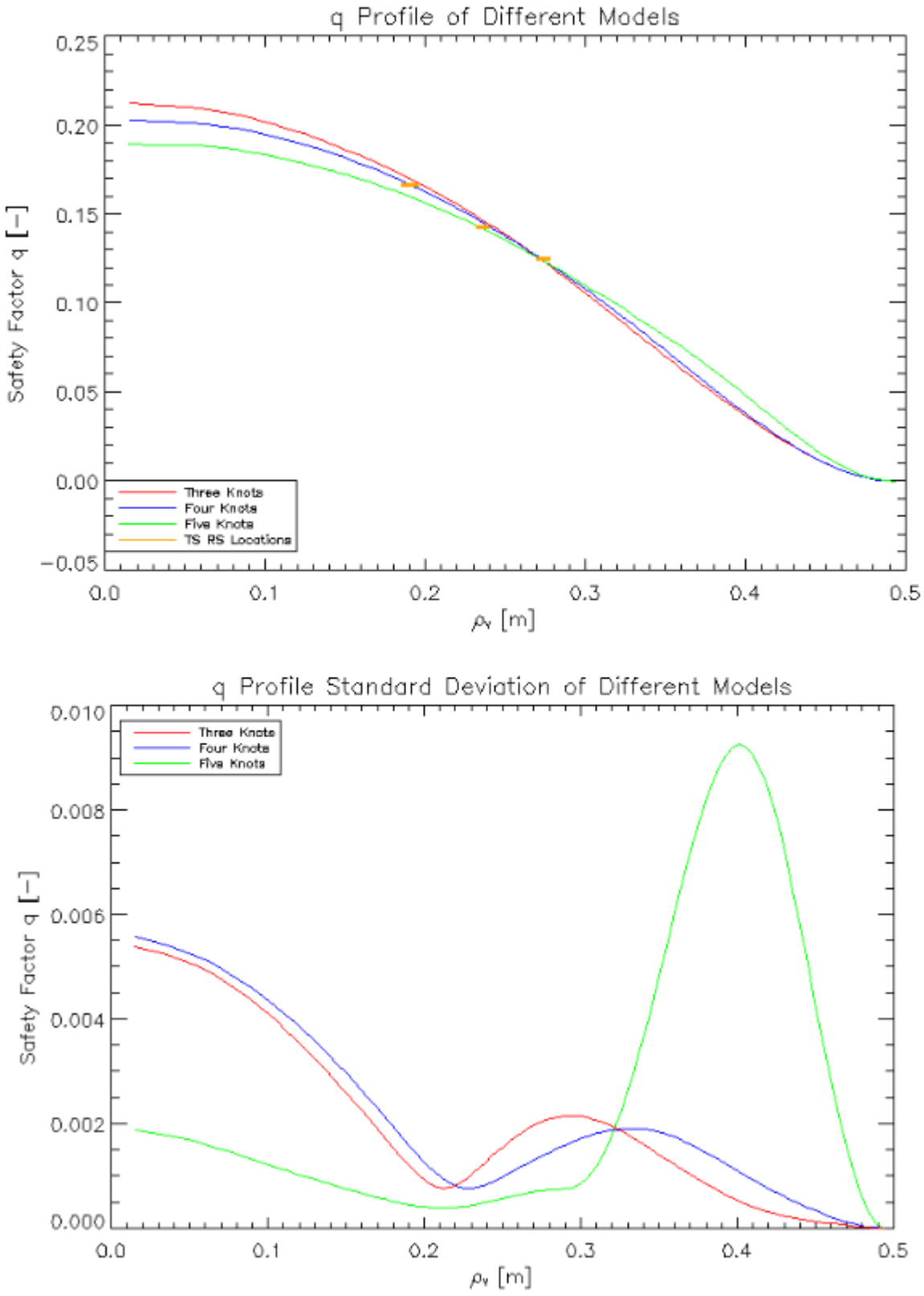

Figure 3.6. q-profile and standard deviation of profile with TS RS location included.

3.3 NBI Suppression of Tearing Modes

Discharges with and without neutral beam injection (NBI) were investigated. It is expected that with NBI present there should be a lowered q(0) due to suppression of the tearing mode. It has been suggested through FIR that there is an inward shift of rational surfaces with NBI [8]. This does not prove that the suppression is due the loss of resonance as a measurement of q(0) is not currently done on MST, but this is a good confirmation. When TS RS locations are included into the reconstruction, the suppression of the resonant tearing mode can just barely resolved as seen in Figure 3.7. The q profile is shown with and without NBI; there is a reduction in q(0) of approximately 0.015 when NBI is present. This is due to the constraint of TS RS on the core,through both the equilibrium constraint as well as the additional knot that is allowed by including TS RS. Only three knots were used on the reconstructions that did not include TS RS this method also produced a reduction in the core with NBI present, giving confirmation to the decrease seen in the four knot model.

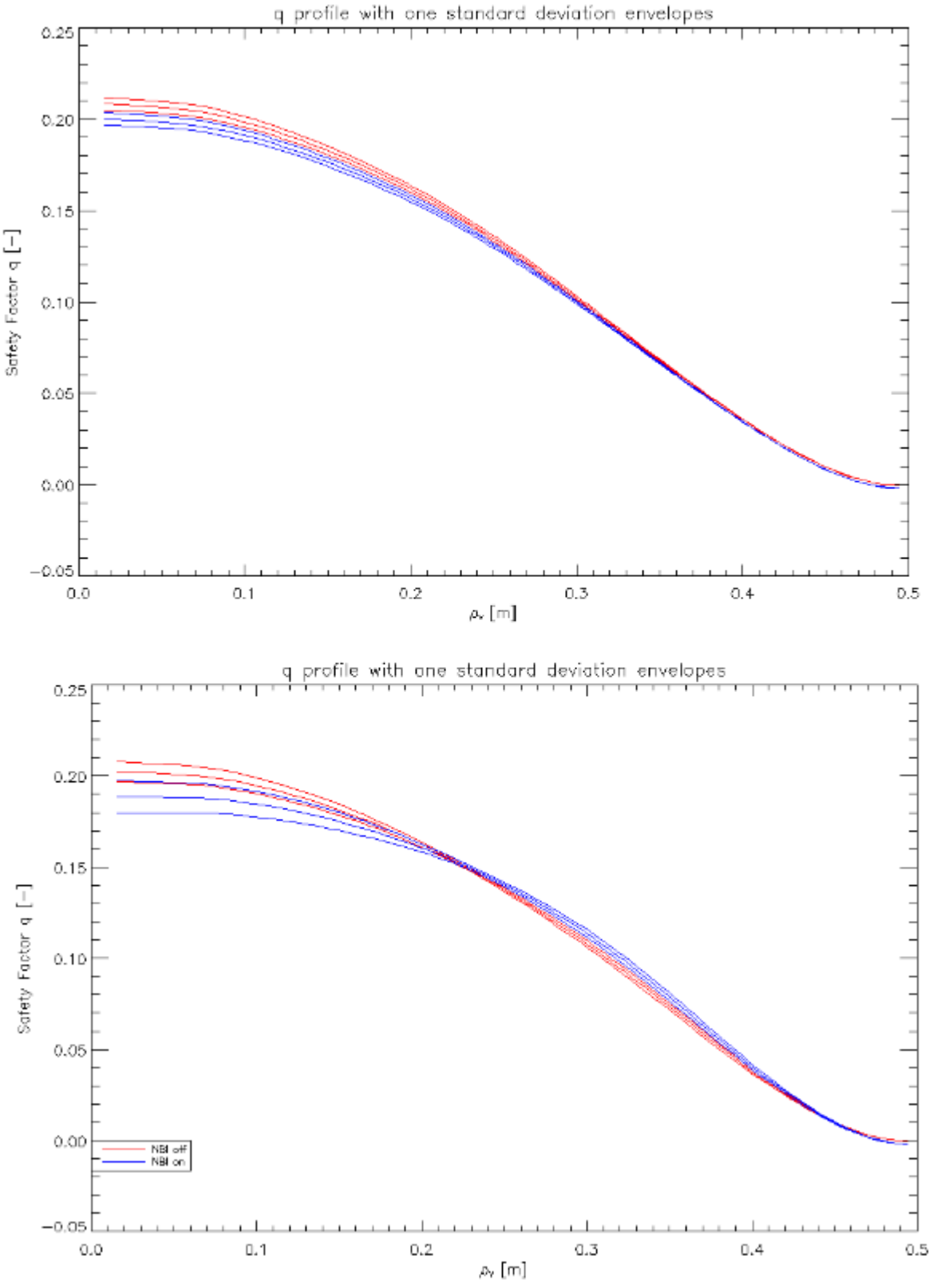

Figure 3.7. q-profile with standard deviation envelopes showing suppression of tearing modes.

Conclusion

The quadratic approximation to back out errors within the equilibrium has been found to be a good first approximation when compared to the errors found through ensembling 1000s of simulated MST discharges. A new diagnostic has been added to the equilibrium reconstruction program MSTfit. This diagnostic uses rational surface locations found from Thomson Scattering temperature fluctuations to constrain the q profile of the equilibrium. The addition of TS RS locations allows for the addition of a knot in the free parameters suggesting that TS RS locations are a good constraint on the reconstruction. The additional knot allows for more structure to be seen in the reconstruction. The suppression of tearing modes with NBI has been suggested using MSTfit.

[1] J. K. Anderson, Measurement of the Electrical Resistivity Profile in the Madison Symmetric Torus, PhD thesis, University of Wisconsin-Madison, 2001.

[2] H. D. Stephens, Electron Temperature Structures Associated With Magnetic Tearing Modes in the Madison Symmetric Torus, PhD Thesis, University of Wisconsin-Madison, 2010.

[3] J. D. Hanson, S. P. Hirshman, S. F. Knowlton, L. L. Lao, E. A. Lazarus, J. M. Shields, V3FIT: a code for three-dimensional equilibrium reconstruction, Nucl. Fusion 49, 2009, 070531

[4] C.S. Jones, J. M. Finn, MHD equilibrium reconstruction in the presence of correlated data, Nucl. Fusion 46, 2006, 335-349

[5] J. Berrino, E. Lazzaro, S. Cirant, G. D'Antona, F. Gandini, E. Minardi, G. Granucci, Electron cyclotron emission temperature fluctuations associated with magnetic islands and real-time identification and control system, Nucl. Fusion 45, 2005, 1350-1361

[6] A. Isayama, Y. Kamada, S. Ide, K. Hamamatsu, T. Oikawa, T. Suzuki, Y. Neyatani, T. Ozeki, Y. Ikeda, K. Kajiwara and the JT-60 team, Complete stabilization of a tearing mode in steady state high β_p H-mode discharges by the first harmonic electron cyclotron heating/current drive on JT-60U, Plasma Phys. Control. Fusion, 42, No 12, 2000 Dec, L37-L45

[7] E. Parke, PhD thesis, to be published, University of Wisconsin-Madison, 2014

[8] Measurement of energetic-particle-driven core magnetic fluctuations and induced fast-ion transport Lin, L. and Ding, W. X. and Brower, D. L. and Koliner, J. J. and Eilerman, S. and Reusch, J. A. and Anderson, J. K. and Nornberg, M. D. and Sarff, J. S. and Waksman, J. and Liu, D., Physics of Plasmas (1994-present), 20, 030701 (2013), DOI:http://dx.doi.org/10.1063/1.4798397

[9] Bevington, Philip R. *Data Reduction and Error Analysis for the Physical Sciences*. New